Appendix

Spin Multiplicity and Potential Curves (Figure 1). The open-shell "triplet" states are specified as having $S_z = 1$ with no relation between the spin up and spin down orbitals. The open-shell "singlet" states are specified as having $S_z = 0$ and no relation between spin up and spin down orbitals. If we had a restricted open-shell triplet and singlet, the Slater determinants would be

$$\Psi_t = \langle \Phi_i \bar{\Phi}_i ... \Phi_{n-1} \bar{\Phi}_{n-1} \Phi_n \Phi_m \rangle \qquad (A\text{-}1)$$

$$\Psi_s = \langle \Phi_i \bar{\Phi}_i ... \Phi_{n-1} \bar{\Phi}_{n-1} \Phi_n \bar{\Phi}_m \rangle \qquad (A\text{-}2)$$

These states have $\langle S^2 \rangle$ and 2 and 1, respectively, since Ψ_t is a true triplet with $S_z = 1$ while Ψ_s is a 50–50 mixture of a true triplet with $S_z = 0$ and a true singlet. However, as shown in Table I, $\langle S^2 \rangle$ for the open-shell "singlet" (Ψ_c) and "triplet" (Ψ_b) states are respectively 1.5 and 2.5. The extra 0.5 above what is required for restricted states (A-1) and (A-2) presumably represents the contribution from a lack of complete identity of spin-paired electrons $\Phi_i \bar{\Phi}_i$ due to the different electron repulsion of the unpaired electrons Φ_n and Φ_m. While the true ground state should be a triplet, the calculated ground state picks up contributions from states of higher multiplicity in an attempt to minimize total energy with a singlet Slater determinantal wave function. In this way the state is modified to include some correlation energy.

For states Ψ_b and Ψ_c (curves b and c of Figure 1), the outer orbitals Φ_n and Φ_m are similar. Thus the energy gap between the

states represents half the energy between the true singlet and triplet biradicals, since Ψ_c is necessarily a 50–50 mixture of these. Presumably when the triplet oxygen atom is transferred to benzene, the intial state formed is the triplet. The presence of the neighboring porphyrin ring with unpaired electrons should cause fast relaxation among the three triplet and one singlet states of curves b and c. However, only from the singlet state will the molecules cross over to form the epoxide product. If the relaxation among the singlet and triplet states is fast compared to the rate of crossing the potential barrier, the effect of spin would be to reduce the rate to $^1/_4$ its value for the singlet alone.

The "potential curve" for the closed-shell singlet, Ψ_a in Figure 1, does not represent any real curve since our calculational method does not require that Ψ_a and Ψ_c be orthogonal. The merger of the a and c potential curves is an artifact of our calculational method and represents the region where the ground state becomes closed shell in character. The true second singlet state should occur at energies above the lowest triplet state—at least at the right end of the diagram where we are dealing with the closed-shell epoxide product. We have indicated on Figure 1 a qualitative guess for the unphysical region of curve a and the form of the true second singlet curve.

The MNDO method has been parameterized to give good ΔH_f for closed-shell molecules. Our potential curves (Figure 1) carry us from an open-shell biradical to a closed-shell product. It is not clear, at this time, whether this method introduces systematic errors along this curve.

Crystal Structure of Aspartame, a Peptide Sweetener

Marcos Hatada,[†] Jarmila Jancarik, Bradford Graves, and Sung-Hou Kim*

Contribution from the Department of Chemistry and Lawrence Berkeley Laboratory, University of California, Berkeley, California 94720. Received October 25, 1984

Abstract: We report on the crystal structure of aspartame, a dipeptide having an intensely sweet taste. The molecule has a molecular formula $C_{14}N_2O_5H_{18} \cdot ^1/_2 H_2O$ and crystallizes in space group $P4_1$ with cell parameters $a = b = 17.685$ (5) Å, and $c = 4.919(2)$ Å, $z = 4$. The final R value is 4.5%. The structure reveals an interesting arrangement of molecules in the crystal, which explains its solution behavior and may be important in designing new and modified sweeteners that will help further our understanding of the structural basis for sweet taste.

Aspartame is a new type of sweetener, about 200 times sweeter than sugar, and is currently widely used as a sugar substitute in beverages and low-calorie foods. The molecule is a methyl ester of the dipeptide L-aspartyl-L-phenylalanine[1] and is sold under the brand name of "NutraSweet" by G. D. Searle and Co. of Skokie, IL.

The molecule in aqueous solution is heat labile and pH sensitive; at 25 °C the optimum pH is 4.2, with a half-life of 260 days, but at higher temperature and pH, the molecule loses its sweet taste and degrades very rapidly to aspartylphenylalanine or its diketopiperazine, then to aspartic acid and phenylalanine. Aspartame is slightly soluble in water (about 5% at 20 °C and pH 7) and sparingly soluble in alcohol. It has a strong tendency to form very fine fibres when crystallized.

Substitution of other amino acids for aspartic acid and phenylalanine showed that aspartic acid is essential for the sweet taste. Furthermore, of the four possible diastereoisomers of aspartame, only the LL isomer was sweet.[2,3]

Though theories on sweet taste are not highly developed, considerable efforts have been directed toward chemical modi-

fication of aspartame and designing new aspartic acid based sweeteners.[3] Examination of many sweet compounds suggests that most of them have an electronegative atom B and a polarized hydrogen donor system A–H with a distance between A and B of about 3 Å[4] and a third and hydrophobic group X at distances of 3.5 and 5.5 Å from A and B, respectively.[5] In aspartame, the A–H:B system is present at the aspartyl residue where $-NH_3^+$ represents A–H and the oxygens of the aspartate sidechain represent B. But there is no candidate for the X group.

Experimental Section

As mentioned earlier, aspartame crystallizes out from most common aqueous and organic solvents as extremely fine fibres, unsuitable for X-ray crystallographic studies. After screening a large number of binary and ternary solvent systems, a suitable aspartame crystal was obtained from a quaternary solvent system: the sample was dissolved to super-

(1) Mazur, R. H.; Schlatter, J. M.; Goldkamp, A. H. *J. Am. Chem. Soc.* **1969**, *91*, 2684.
(2) Mazur, R. H. Symposium: "Sweeteners"; Inglett G. E., Ed.; Avi Publishing Co.: Westport, CT, 1974; p 159.
(3) Mazur, R. H.; Goldkamp, A. H.; James, P. A.; Schlatter, J. M. *J. Med. Chem.* **1970**, *13*, 1217.
(4) Shallenberger, R. S.; Acree, T. E. *Nature (London)* **1967**, *216*, 480.
(5) Kier, L. B. *J. Pharm. Sci.* **1972**, *61*, 1394.

Table I. Atomic Coordinates: Aspartame

atom	X/A	Y/B	Z/C
N1	0.1630 (2)	−0.0488 (2)	0.2983 (15)
CA1	0.2329 (3)	−0.0330 (3)	0.1434 (14)
CB1	0.2400 (3)	0.0513 (3)	0.0765 (13)
CG1	0.1843 (3)	0.0789 (4)	−0.1400 (16)
OD1	0.1373 (2)	0.0326 (2)	−0.2257 (14)
OD2	0.1904 (2)	0.1438 (3)	−0.2245 (15)
C1	0.3001 (3)	−0.0589 (3)	0.3065 (18)
O1	0.2991 (2)	−0.0580 (2)	0.5587 (13)
N2	0.3587 (3)	−0.0824 (3)	0.1632 (15)
CA2	0.4275 (3)	−0.1110 (3)	0.2943 (17)
CB2	0.4162 (3)	−0.1918 (3)	0.4005 (19)
CG22	0.3244 (4)	−0.2593 (4)	0.0916 (22)
CG23	0.3080 (6)	−0.3105 (6)	−0.1104 (24)
CG24	0.3653 (8)	−0.3546 (5)	−0.2202 (26)
CG25	0.4388 (6)	−0.3467 (5)	−0.1313 (24)
CG26	0.4557 (4)	−0.2927 (4)	0.0709 (23)
CG21	0.3984 (4)	−0.2491 (3)	0.1840 (20)
C2	0.4919 (4)	−0.1028 (4)	0.1017 (19)
O21	0.4894 (2)	−0.0711 (3)	−0.1132 (14)
O22	0.5543 (2)	−0.1348 (2)	0.1984 (14)
CM2	0.6200 (3)	−0.1312 (4)	0.0267 (22)
OX	0.0142 (12)	−0.0142 (12)	0.0132 (166)
HN11	0.1126	−0.0425	0.1713
HN12	0.1570	−0.1118	0.3456
HN13	0.1602	−0.0137	0.4333
HCA1	0.2293	−0.0629	−0.0183
HB11	0.2912	0.0564	−0.0319
HB12	0.2279	0.0711	0.2282
HN2	0.3618	−0.0857	−0.0207
HCA2	0.4409	−0.0635	0.4409
HB21	0.3676	−0.1893	0.5239
HB22	0.4610	−0.2052	0.4797
HG22	0.2818	−0.2271	0.1596
HG23	0.2577	−0.3183	−0.1995
HG24	0.3465	−0.3961	−0.3507
HG25	0.4815	−0.3843	−0.1614
HG26	0.5086	−0.2760	0.0932
HM21	0.6536	−0.0863	0.0462
HM22	0.6569	−0.1569	0.1166
HM23	0.6148	−0.1457	−0.1119

Figure 1. The chemical structure and numbering system of aspartame. Bond lengths and angles in aspartame. The average standard deviation is 0.008 Å for the bond lengths and 0.6° for the bond angles.

Figure 2. An ORTEP drawing of the aspartame molecule with one water molecule. Torsion angles along the dipeptide backbone are indicated. These are formed by using only backbone atoms, and in case of ambiguity an atom name is given in parentheses to help define the torsion angle.
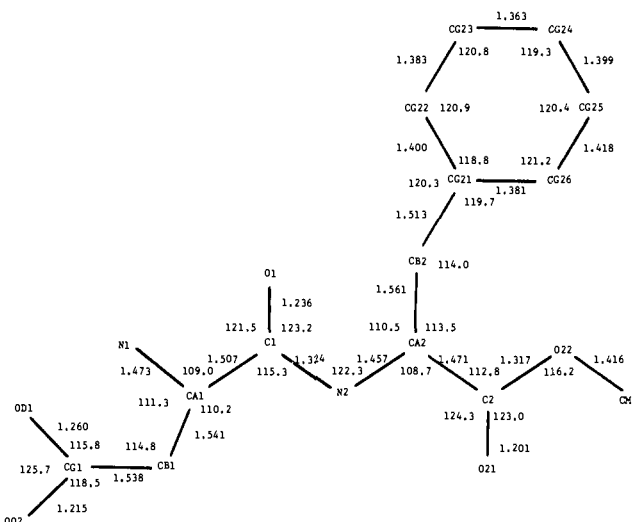
saturation in 0.5 mL of double-distilled water by heating the solution to 40 °C for about 5 min; to this solution was added an equal volume of an aqueous solution containing 20% ethanol, 20% acetone, and 10% Me₂SO by volume. Needle-shaped crystals appeared after 24 h and were allowed to grow for 2 weeks.

Aspartame crystallizes in the tetragonal space group $P4_1$ with unit cell parameters $a = b = 17.685$ (5) Å, $c = 4.919$ (2) Å. The four molecules in the unit cell result in a calculated density of 1.310 gm/cm³. Three-dimensional X-ray diffraction data were collected on a needle-shaped crystal 0.07 × 0.08 × 0.60 mm in size, using graphite monochromatized Mo Kα radiation. A total of 1095 unique reflections was collected for a 2θ range from 5° to 45°. Of these, 899 had intensities greater than twice their estimated standard deviations.
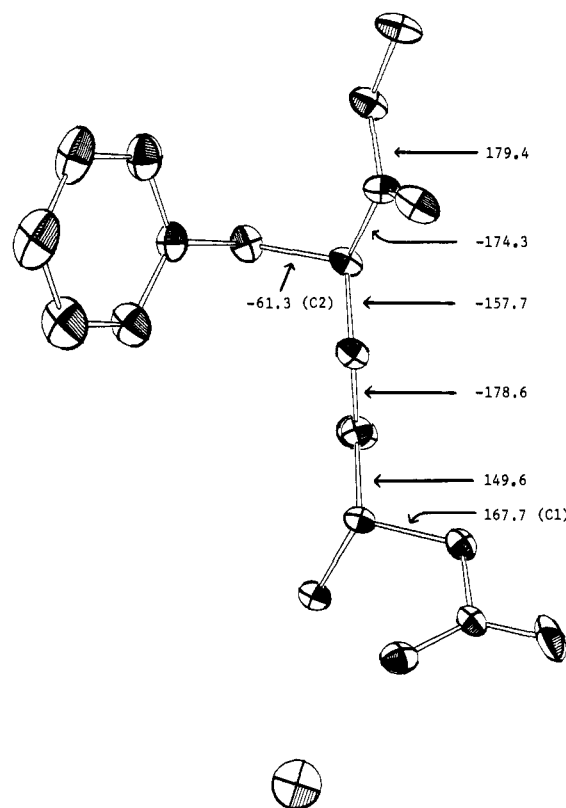
The crystal structure was determined by a direct methods procedure[6] with the MULTAN program system.[7] After a few cycles of full-matrix least-squares refinement of non-hydrogen atoms with the SHELX program,[8] a difference Fourier map revealed all hydrogen atoms except those on the phenylalanine ring. Calculated positions for the ring hydrogens were included in the subsequent refinement. Further full-matrix least-squares refinement, followed by calculation of another difference Fourier map, revealed one disordered (50% occupancy) water molecule. The final R value is 4.5%, and a list of atomic coordinates can be found in Table I.

Discussion

Figure 1 shows the chemical structure of aspartame and the numbering system used in this work. Figure 1 also includes the final values for bond lengths and angles. The bond distances and angles are all within normal limits for this type of molecule. Figure

2 shows an ORTEP drawing[9] of the aspartame molecule and the disordered water molecule. Also shown in this figure are torsion angles along the dipeptide backbone. The conformations of the bonds in the dipeptide are all very close to trans conformation. The N-terminus is positively charged, but the aspartate side chain is negatively charged; thus the molecule is zwitterionic and highly hydrophilic on the aspartyl side. The phenylalanine side of the molecule, on the other hand, is highly hydrophobic because the negative charge, normally present at the C-terminus, is eliminated by formation of the methyl ester. This clear segregation of the

(6) Karle, J.; Hauptman, H. *Acta Crystallogr.* **1953** 6, 473.

(7) Main, P.; Friske, S. J.; Hull, S. E.; Lessinger, L.; Germain, G.; Declerco, J. P.; Woolfson, M. M. MULTAN80, University of York, England, 1980.

(8) Sheldrick, G. M. SHELX76, University Chemical Laboratory, Cambridge, England, 1976.

(9) Johnson, C. K. ORTEP, Report ORNL-5138, Oak Ridge National Laboratory, TN, 1976.

Crystal Structure of Aspartame

J. Am. Chem. Soc., Vol. 107, No. 14, 1985 4281
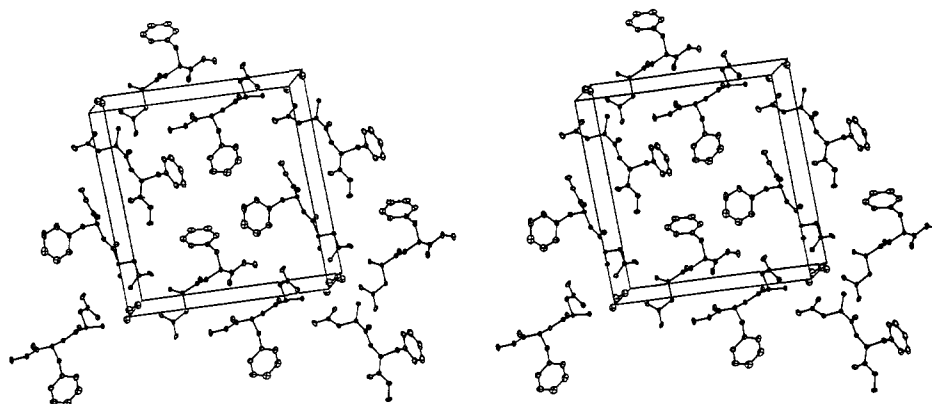
Figure 3. A stereo drawing of the molecular packing in an aspartame crystal. The short axis is the crystallographic c axis; a and b axes are approximately horizontal and vertical, respectively.
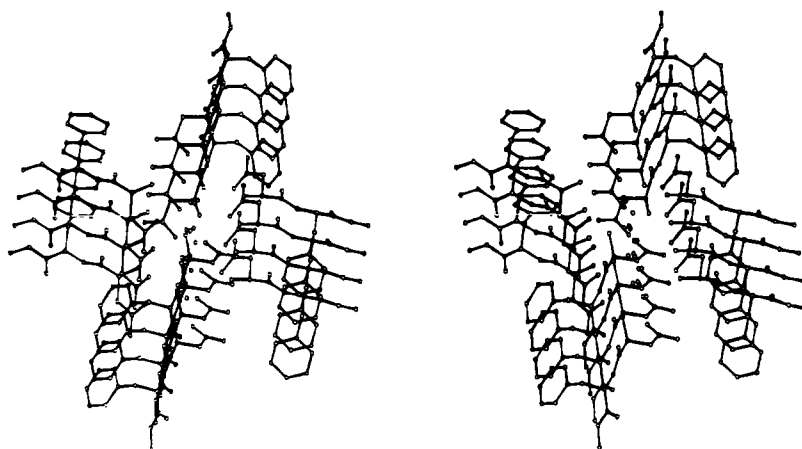
Figure 4. A stereo drawing of a columnar structure of aspartame molecules: An extensive and elaborate hydrogen bond network is interconnecting zwiterionic N-terminal ends of the molecules and water molecules forming an infinite column along a 4_1 axis. The outer surface of the column is highly hydrophobic due to phenyl and methyl groups of the C-terminus of the molecule.
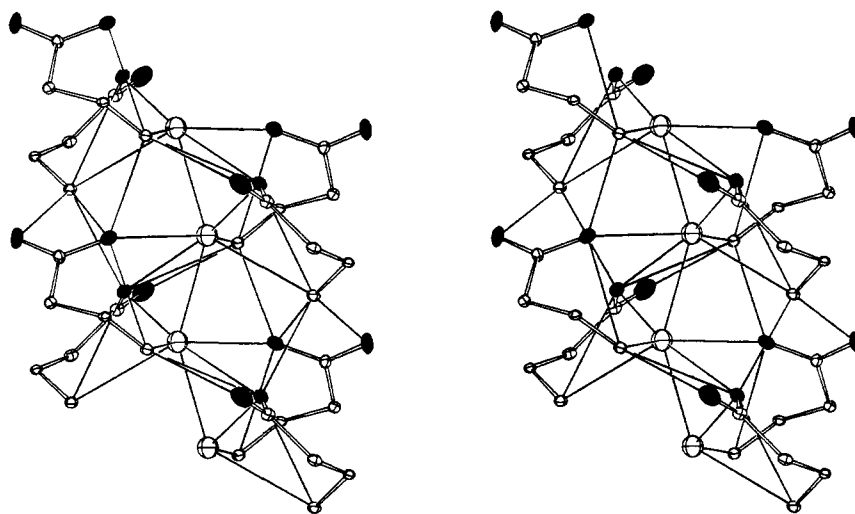
Figure 5. A stereo drawing depicting the hydrogen-bonding scheme along the hydrophilic core. The crystallographic c axis is vertical and two unit cells are shown in this direction in order to obtain a complete picture of the hydrogen bonds involving the water molecules. Only one of the two pairs of water molecules is present. The hydrogen-bonding scheme for the other pair of water molecules is identical with this. For clarity, only the N-terminal fragment of aspartame (N1-CA1-CB1-CG1-OD1 and OD2) is included and the ellipsoids for OD1 and OD2 have been shaded.

hydrophobic and hydrophilic segments of the molecule results in an interesting molecular organization in the crystal.

The molecular packing in the crystal is shown in Figure 3. At each corner of the unit cell there is a clustering of four N-terminal charged groups per unit cell, linked to each other by the disordered water molecule through many hydrogen bonds, thus forming an infinite column with a hydrophilic core surrounded by a hydrophobic surface (Figure 4). Four such columns come together in contact at the center of the unit cell, stabilized by the hydro-

phobic interaction of phenyl groups. The shortest contact distances between phenyl rings are 3.5 Å for a stacking type interaction and 4.0 Å for an edge on interaction. The formation of this columnar structure with hydrophobic surfaces explains the tendency for fibre formation and low water solubility of aspartame; despite that one-half of the molecule is highly hydrophilic.

The hydrogen-bonding scheme through the hydrophilic core is very elaborate and is dominated by hydrogen bonds to and from the water molecules. In the crystal we have the unusual situation

Table II. Hydrogen Bond Distances and Angles in Aspartame

D–H		A^a	D–A	H–A	D–H–A
N1	HN11	OD1[1]	2.99	2.40	112
		OX3[1]	3.04	1.97	166
		OX3[2]	2.86	2.06	128
N1	HN12	OD1[4]	3.00	2.41	110
		OD2[4]	2.76	1.85	159
N1	HN13	OD1[6]	2.79	1.91	161
OX3		OD1[1]	2.61		
		OX3[5]	2.56		
OX3		OD1[2]	2.80		
		OD1[3]	2.99		

^{a} Symmetry code: (1) x, y, z; (2) $-y, x, z + \frac{1}{4}$; (3) $-x, -y, z + \frac{1}{2}$; (4) $y, -x, z + \frac{3}{4}$; (5) $-x, -y, z - \frac{1}{2}$; (6) $x, y, z + 1$.

that the four symmetry-related positions of the water molecules are too close to exist simultaneously in one unit cell. Thus, in any given unit cell either one pair or the other is present. This is the reason for the water molecule having 50% occupancy. In either case the hydrogen-bonding scheme obviously is equivalent. As can be seen in Figure 5, the water molecules apparently are involved in seven hydrogen-bonding contacts. The water molecule acts as a donor in four instances (to three different OD1 atoms and to the neighboring water oxygen atom through bifurcated hydrogen bonds) and as an acceptor in three other directions (from two N1 positions and the other neighboring water molecule). The only other available donor is the terminal $-NH_3^+$ group and it

participates in six hydrogen bonds (to three different OD1 atoms, one water molecule and to an OD2 atom through bifurcated hydrogen bonds). One of the hydrogen bonds between N1 and OD1 is an intramolecular hydrogen bond. Thus, the extensive and elaborate hydrogen bonding is interconnecting aspartame molecules to form a long column with hydrophobic surface. Distance and angles associated with all of the hydrogen bonds are reported in Table II.

At the present time little is known about the sweet receptors on the human tongue, and nothing is known about what form of aspartame is recognized by these receptors. But intense efforts are being directed toward the chemical modification of aspartame and the design of aspartame-like molecules not only to understand the chemical and structural determinants of the sweet taste but also to find a better sweetener. The detailed three-dimensional structure of aspartame and its columnar polymeric arrangement provide a reasonable explanation for unexpected low water solubility and fibre-forming tendency of the molecule, and it may provide some important new insights for these purposes.

In Vitro Reaction of the Carcinogen Chromate with Cellular Thiols and Carboxylic Acids

P. H. Connett[1] and K. E. Wetterhahn*

Contribution from the Department of Chemistry, Dartmouth College, Hanover, New Hampshire 03755. Received November 8, 1984

Abstract: Since a key step in the carcinogenicity and toxicity of chromium(VI) compounds is intracellular reduction to chromium(III), we have examined the interaction of chromium(VI) with a series of low molecular weight cellular reductants and model compounds at physiological pH. The reduction of chromium(VI) at physiological pH was found to be under kinetic rather than thermodynamic control. Only ascorbate and those reductants containing a thiol group were capable of reducing chromium(VI) at a significant rate at pH 7.4 (1 M Tris–HCl). The kinetics describing the reaction of chromium(VI) with the various thiols could be separated into four categories: (a) glutathione showed clear spectral evidence for the formation of a chromium(VI) thioester in a rapid pre-equilibrium step, followed by a slower redox step involving reaction of the chromium(VI) thioester with a second molecule of thiol; (b) cysteine ethyl ester, cysteine, cysteamine, coenzyme M, homocysteine, N-acetylcysteine, coenzyme A, mercaptoethanol, and thioglycolate showed formation of a chromium(VI) thioester followed by a redox step involving reaction of the thioester with a second molecule of thiol with kinetics consistent with the steady-state approximation; (c) penicillamine, dithiothreitol, 2,3-dimercaptosuccinate, thiolactate, and thiomalate showed rate-determining formation of the chromium(VI) thioester; and (d) unithiol and dihydrolipoate showed the formation of a chromium(VI) thioester in a rapid pre-equilibrium step, followed by a unimolecular redox reaction of the thioester, although there was no spectral evidence for thioester formation. Of possible biological importance is the fact that glutathione, the most abundant intracellular thiol, appeared in the first category. The rapid formation of the chromium(VI) glutathione thioester, followed by its slow reduction, may well prolong the lifetime of chromium(VI) in the cell and promote its interaction with cellular macromolecules. Brønsted plots showed that the second-order rate constants for the first step of the thiol–chromium(VI) reaction, formation of the chromium(VI) thioester, were inversely related to the pK_a's of the thiol groups. At pH 7.4, it appears that chromate, CrO_4^{2-}, is attacked by the un-ionized thiol which transfers a proton to an oxygen atom of the chromate as part of the rate-limiting step and that the subsequent loss of the hydroxide ligand, OH^-, is facilitated by protonation in the case of thiols containing a free amino group.

In recent years, several studies have reviewed the toxicity and carcinogenicity of chromium compounds.[2–4] Epidemiological and

animal studies, as well as in vitro mutagencity assays,[5] indicate that chromium(VI) compounds pose serious dangers to biological